Eur Radiol (2004) 14:783–791
DOI 10.1007/s00330-004-2249-9

Mathias Goyen
Susanne C. Goehde
Christoph U. Herborn
Peter Hunold
Florian M. Vogt
Elke R. Gizewski
Thomas C. Lauenstein
Waleed Ajaj
Michael Forsting
Jörg F. Debatin
Stefan G. Ruehm

MR-based full-body preventative cardiovascular and tumor imaging: technique and preliminary experience

Received: 15 September 2003
Revised: 31 December 2003
Accepted: 9 January 2004
Published online: 13 February 2004

M. Goyen (✉) · S. C. Goehde
C. U. Herborn · P. Hunold · F. M. Vogt
E. R. Gizewski · T. C. Lauenstein
W. Ajaj · M. Forsting · J. F. Debatin
S. G. Ruehm
Department of Diagnostic
and Interventional Radiology,
University Hospital Essen,
Hufelandstrasse 55, 45147 Essen,
Germany
e-mail: mathias.goyen@uni-essen.de
Tel.: +49-201-7231501
Fax: +49-201-7231548

Abstract Recent improvements in hardware and software, lack of side effects, as well as diagnostic accuracy make magnetic resonance imaging a natural candidate for preventative imaging. Thus, the purpose of the study was to evaluate the feasibility of a comprehensive 60-min MR-based screening examination in healthy volunteers and a limited number of patients with known target disease. In ten healthy volunteers (7 men, 3 women; mean age, 32.4 years) and five patients (4 men, 1 woman; mean age, 56.2 years) with proven target disease we evaluated the performance of a comprehensive MR screening strategy by combining well-established organ-based MR examination components encompassing the brain, the arterial system, the heart, the lungs, and the colon. All ten volunteers and five patients tolerated the comprehensive MR examination well. The mean in-room time was 63 min. In one volunteer, insufficient colonic cleansing on the part of the volunteer diminished the diagnostic reliability of MR colonography. All remaining components of the comprehensive MR examination were considered diagnostic in all volunteers and patients. In the five patients, the examination revealed the known pathologies [aneurysm of the anterior communicating artery (n=1), renal artery stenosis (n=1), myocardial infarct (n=1), and colonic polyp (n=2)]. The outlined MR screening strategy encompassing the brain, the arterial system, the heart, the lung, and the colon is feasible. Further studies have to show that MR-based screening programs are cost-effective in terms of the life-years saved.

Keywords Screening · Magnetic resonance imaging · Whole-body MR angiography · MR colonography · Colonic cancer · Cardiovascular disease

Introduction

To date, radiological approaches to screening have included chest radiography for tuberculosis screening throughout Europe in the 1960s and 1970s [1, 2] and more recently low-dose computed tomography (CT) for the detection of lung cancer [3–5]. With the availability of multislice CT, elective full-body CT screening services have become available for health-conscious individuals [6]. However, all of these approaches are burdened by considerable exposure to ionizing radiation. The dangers associated with higher radiation doses have motivated the Federal Drug Administration (FDA) of the United States to issue "radiation alerts" [7]. The European Union prohibits examinations using ionizing radiation for screening purposes with the exception of mammography [8].

Lack of ionizing radiation and contrast agents void of any nephrotoxicity, in conjunction with high diagnostic accuracy based on unsurpassed soft-tissue contrast as well as high spatial and temporal resolution, make magnetic resonance (MR) imaging a natural candidate for preventa-

tive imaging. To date, cost concerns and lengthy data acquisition times have prohibited its use in this regard. Building on the highest-performance gradient hardware and new whole-body MR imaging concepts [9–12], we have developed an MR-based screening protocol capable of assessing the central nervous system, the cardiovascular system, the lung, as well as the colon. Theoretically, the exam could be completed within 1 h. The purpose of this study was to prove the feasibility of such a comprehensive 60-min MR screening strategy by combining well-established organ-based MR examination components.

Materials and methods

Subjects

Within a 5-week period (February–March 2002) a comprehensive MR examination was performed on ten healthy volunteers (7 men, 3 women; mean age, 32.4 years) and five patients (4 men, 1 woman; mean age, 56.2 years) with proven disease in one of the target organs of the screening examination [aneurysm of the anterior communicating artery (n=1), renal artery stenosis (n=1), myocardial infarct (n=1), and colonic polyp (n=2)].

The study was performed according to good clinical practice (GCP) rules and was approved by the local ethical committee. Written informed consent was obtained from all patients, who were not charged for the examination. Vital signs and adverse reactions were monitored for up to 24 h following the MR examination.

MR imaging

All imaging was performed on a 1.5-T MR system (Magnetom Sonata, Siemens Medical Systems, Erlangen, Germany), equipped with a high-performance gradient system characterized by an amplitude of 40 mT/m and a slew rate of 200 mT/m/ms (MR Ease Software 15 A). To enable whole-body coverage, all volunteers were examined on a fully MR-compatible rolling table platform (Angio*SURF*, MR-Innovation GmbH, Essen, Germany) [12, 13]. The platform is 240 cm long and moves on seven pairs of roller bearings, which are anchored within the existing patient table. Up to six 3D data sets with a craniocaudal coverage of 380 mm each can be collected in immediate succession. Markers permit adjustment to the desired field of view (FOV). Signal reception is accomplished using posteriorly located spine coils and an anteriorly placed torso phased-array coil which rests in a height-adjustable coil holder. Thus, data for all six stations are collected with the same stationary coil set positioned in the isocenter of the magnet.

Paramagnetic contrast agent was administered intravenously on two occasions: once for imaging of the arterial vascular tree [0.2 mmol/kg body weight (bw)] [14] and a second time for MR colonography (0.1 mmol/kg bw) [15]. The total dose amounted to 0.3 mmol/kg bw. Gadobutrol (Gadovist 1.0, Schering AG, Berlin, Germany), an extracellular neutral gadolinium chelate with a concentration of 1 mol Gd/l was chosen based on its beneficial MR angiography imaging characteristics [16, 17]. For contrast administration, a 19-G plastic i.v. line was placed in the right antecubital vein. The MR examination can be subdivided into four parts. Specific imaging parameters are summarized in Tables 1, 2, 3, 4.

For MR imaging of the brain (Table 1), volunteers and patients were placed head first within the bore of the magnet and examined in the supine position. The cerebrum was assessed by fast T1-weighted and T2-weighted spin-echo sequences, fluid-attenuated inversion recovery (FLAIR) imaging as well as diffusion-weighted imaging. The intracerebral arterial system was directly visualized by axial 3D time-of-flight (TOF) MR angiography.

For whole-body MR angiography (Table 2), the volunteers and patients were placed with their feet first within the bore of the

Table 1 Cerebral MR imaging (*TR* repetition time, *TE* echo time, *FOV* field of view, *FLAIR* fluid-attenuated inversion recovery)

T1-weighted imaging	
TR	190 ms
TE	4.8 ms
FOV	230 mm
Plane orientation	Transverse
Flip angle	70°
Slice thickness	6 mm
No. of slices	19
Acquisition time	29 s
Spatial resolution	1.1×0.9×6.0 mm^3
Matrix	256
T2-weighted imaging	
TR	4,800 ms
TE	105 ms
FOV	230 mm
Plane orientation	Transverse
Flip angle	150°
Slice thickness	6 mm
No. of slices	19
Acquisition time	50 s
Spatial resolution	1.1×0.9×6.0 mm^3
Matrix	256
Diffusion 2D TRACE	
TR	180 ms
TE	118 ms
FOV	230 mm
Plane orientation	Transverse
Slice thickness	6 mm
No. of slices	19
Acquisition time	88 s
Spatial resolution	2.6×1.8×6.0 mm^3
Matrix	128
T2-weighted FLAIR	
TR	8,430 ms
TE	119 ms
FOV	230 mm
Plane orientation	Transverse
Flip angle	150°
Slice thickness	6 mm
No. of slices	19
Acquisition time	2 min 33 s
Spatial resolution	1.0×0.9×6.0 mm^3
Matrix	256
TOF	
TR	40 ms
TE	7.5 ms
FOV	200 mm
Plane orientation	Transverse
Flip angle	25°
Slice thickness	1 mm
No. of slices	32 per slab (3 slabs)
Acquisition time	5 min 35 s
Spatial resolution	0.8×0.4×1.0 mm^3
Matrix	512

Table 2 Whole-body MR angiography (*FISP* fast imaging with steady-state precession, *FLASH* fast low-angle shot)

TrueFISP moving scout	
TR	4.45 ms
TE	2.22 ms
FOV	400 mm
Flip angle	70°
Slice thickness	10 mm
No. of slices	6
Acquisition time	9 s
Spatial resolution	3.1×1.6×10 mm^3
Matrix	256
Test bolus	
TR	1,000 ms
TE	1.58 ms
FOV	400 mm
Plane orientation	Coronal
Flip angle	8°
Slice thickness	10 mm
No. of slices	60
Acquisition time	60 s
Spatial resolution	3.0×1.6×10 mm^3
Matrix	256
Contrast injection	Test bolus, 1 ml gadobutrol; flow, 1.3 ml/s+30 ml NaCl; flow, 1.3 ml/s; scan, proximal third descending aorta
Contrast-enhanced 3D FLASH	
TR	2.2 ms
TE	0.74 ms
FOV	390 mm
Plane orientation	Coronal
Flip angle	20°
Slice thickness	1.5
No. of slices	64
Acquisition time	12 s
Spatial resolution	1.8×1.5×1.5 mm^3
Matrix	256
Contrast injection	0.2 mmol/kg bw gadobutrol, diluted with NaCl to 60 ml; biphasic injection protocol, 1.3 ml/s for the first half, 0.7 ml/s for the second half of the bolus+30 ml NaCl; flow, 1.3 ml/s

Table 3 Cardiac MR imaging (*HASTE* half-Fourier single-shot turbo spin-echo)

HASTE	
TR	800 ms
TE	23 ms
FOV	350 mm
Plane orientation	Transverse
Flip angle	160°
Slice thickness	8 mm
No. of slices	30
Acquisition time	24 s
Spatial resolution	2.4×1.4×8.0 mm^3
Matrix	512
TrueFISP 4- chamber	
TR	47.4 ms
TE	1.58 ms
FOV	340 mm
Flip angle	60°
Slice thickness	8 mm
No. of phases	15
Acquisition time	11 s
Spatial resolution	1.7×1.3×8.0 mm^3
Matrix	256
Volumetry shared-phases	
TR	46.88 ms
TE	1.46 ms
FOV	390 mm
Flip angle	60°
Slice thickness	8 mm
No. of slices/phases/segments	3/13/32
Acquisition time	12 s
Spatial resolution	2.5×1.5×8.0 mm^3
Matrix	256
Late enhancement short-axis 3D	
TR	556.5 ms
TE	1.34 ms
FOV	400 mm
Plane orientation	Transverse
Flip angle	25°
Slice thickness	5 mm
No. of slices	30
Acquisition time	22 s
Spatial resolution	1.6×1.6×5.0 mm^3
Matrix	256
Late enhancement long-axis 2D	
TR	690 ms
TE	4.38 ms
FOV	320 mm
Plane orientation	Transverse
Flip angle	25°
Slice thickness	8 mm
No. of slices	1
Acquisition time	10 s
Spatial resolution	1.6×1.3×8.0 mm^3
Matrix	256

magnet and examined in the supine position on the Angio*SURF* system. Whole-body MR angiography is based on the acquisition of five slightly overlapping 3D data sets acquired in immediate succession. The first data set covers the aortic arch and the supra-aortic vessels, while the second covers the descending aorta with its major branches including the renal and mesenteric arteries. The third data set displays the pelvic arteries, while the last two cover the arteries of the thighs and calves, respectively. Based on a true fast imaging with steady-state precession (FISP)-scout protocol and following determination of the contrast agent travel time to the aortic arch with a test bolus, slightly overlapping 3D data sets were collected using a 3D fast low-angle shot (FLASH) sequence (acquisition time 12 s). A 2-cm overlap at each station's end resulted in a craniocaudal coverage of 174 cm. For MR angiography, gadobutrol was administered at a weight-adjusted dosage of 0.2 mmol/kg bw, diluted with normal saline to a total volume of 60 ml. Contrast agent was injected automatically (MR Spectris, Medrad, Pittsburgh, PA) using a biphasic protocol: the first half was injected at a rate of 1.3 ml/s, while the second half was administered at a rate of 0.7 ml/s, followed by a 20-ml saline flush.

The heart (Table 3) was examined head first in the supine position. Axial half-Fourier single-shot turbo spin-echo (HASTE) im-

Table 4 MR colonography (*VIBE* volume interpolated breath-hold examination)

VIBE 3 measurements	Fat-sat
TR	3.10 ms
TE	1.17 ms
FOV	400 mm
Plane orientation	Coronal
Flip angle	12°
Slice thickness	1.6 mm
No. of slices	96
Acquisition time	23 s
Spatial resolution	2.1×1.6×1.6 mm^3
Matrix	256
Contrast administration	0.1 mmol/kg bw gadobutrol; flow. 3 ml/s+30 ml NaCl, start of first scan 60 s postcontrast administration
T1-weighted postcontrast	
TR	100 ms
TE	4.57 ms
FOV	350 mm
Plane orientation	Transverse
Flip angle	70°
Slice thickness	10 mm
No. of slices	27
Acquisition time	54 s
Spatial resolution	1.5×1.4×10.0 mm^3
Matrix	256

aging was performed to assess cardiac morphology as well as the pulmonary parenchyma. Subsequent functional assessment of the heart was based on segmented true FISP-cine measurements. Each 8-mm slice along the long and short axis as well as along the left ventricular outflow tract was collected within the confines of a single breath-hold. A 3D segmented inversion recovery turbo gradient-echo sequence, collected in both the short and long axis about 20 min after contrast administration for whole-body MR angiography, was assessed for areas of "late enhancement" denoting myocardial infarction.

For MR colonography (Table 4), the volunteers and patients were placed head first in the prone position. All subjects had undergone standard preparation for bowel cleansing on the previous day. To minimize peristaltic bowel motion during the examination, 40 mg of scopolamine (Buscopan, Boehringer Ingelheim, Germany) was injected intravenously. Following placement of a rectal enema tube, the colon was filled with 1,500–2,500 ml of warm tap water. After the collection of a "precontrast" volume interpolated breath-hold examination (VIBE) gradient-echo data set, 0.1 mmol/kg bw gadobutrol was administered at a rate of 3.0 ml/s. After a delay of 60 and 90 s, respectively, the 3D acquisition was repeated. Each 3D MR colonography data set was collected with a breath-hold of 23 s.

Image and data analysis

The "in-room" time, defined as the time-span between the patient entering the MR room for positioning and the patient leaving the MR room, was determined for all volunteers and patients. All imaging data were analyzed on a workstation (Virtuoso, Siemens Medical Systems, Erlangen, Germany), which permitted 2D, 3D, and cine-loop viewing and rendered maximum intensity projections (MIP) as well as multiplanar reformations (MPRs).

The MR data sets of the brain were reviewed by a board-certified radiologist with subspecialty training in neuroradiology (MF). For analysis of the whole-body MR angiography examinations, the arterial tree was divided into 30 segments. Each segment was analyzed by a board-certified radiologist experienced in MR angiography (SGR) regarding the presence of vascular disease, defined as: (a) luminal narrowing exceeding 50% on the basis of the most severe reduction of the arterial diameter compared with the most normal-appearing segment proximal or distal to the area of arterial compromise, (b) arterial occlusion, or (c) aneurysmal disease.

MR data sets of the chest encompassing the lung and the heart were reviewed by an experienced radiologist with special training in cardiac MR imaging (PH). MR colonography data sets were analyzed by a board-certified radiologist with special training in gastrointestinal MR imaging (JFD). For analysis the colon was divided into five segments (rectum, sigmoid colon, descending colon, transverse colon, ascending colon). The lumen of the colon was searched for the presence of enhancing colorectal masses. If identified, their location and size were recorded. Furthermore, the colon was screened for diverticular disease. The contrast-enhanced abdominal data sets were further assessed for the presence of renal, hepatic, adrenal, or retroperitoneal disease.

Results

All ten volunteers and five patients tolerated the comprehensive MR examination well. The mean in-room time

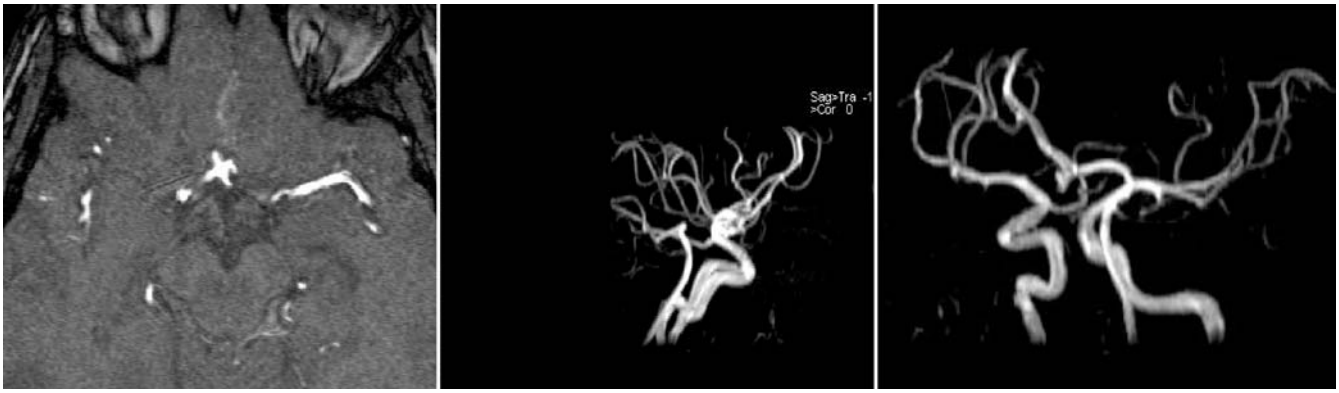

Fig. 1 MR imaging of the brain in a 73-year-old male patient with known aneurysmal disease: the source image as well as the maximum intensity projection show an aneurysm of the anterior communicating artery (4 mm)

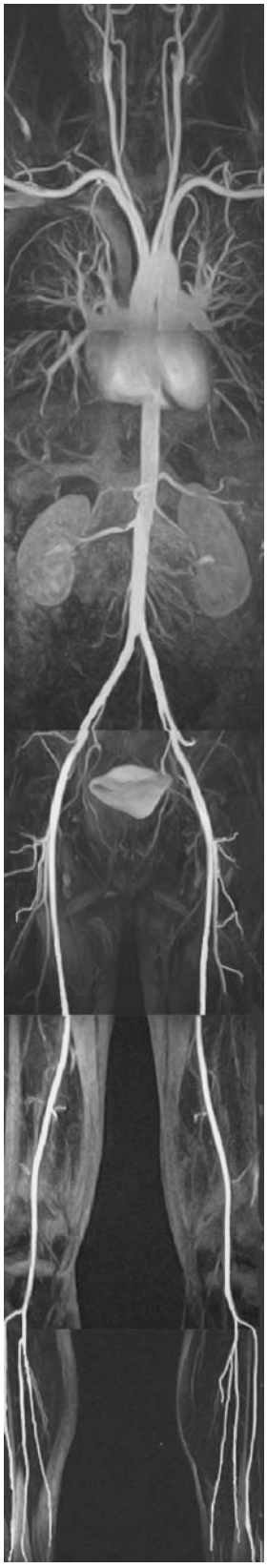

Fig. 2 Angio*SURF*-based whole-body 3D MR angiogram of a 42-year-old male patient with hypertension. The exam consists of five slightly overlapping 3D data sets collected over 72 s. The acquisition time for each 3D data set amounts to 12 s. During a 3-s acquisition break, the table is manually repositioned to the center of the subsequent image volume. With five successive acquisitions, craniocaudal coverage thus extended over 176 cm, while the total data acquisition time amounted to 72 s

for all volunteers and patients was 63.2 min, ranging between 58.6 and 69.2 min. There were no adverse effects associated with the MR examination or the administration of the contrast agent. In one volunteer, insufficient colonic cleansing on the part of the volunteer diminished the diagnostic reliability of MR colonography. All remaining components of the comprehensive MR examination were considered diagnostic in all volunteers and patients.

MR imaging of the brain

The MR data sets of the brain permitted diagnostic analysis of the cerebral morphology. In the patient with known aneurysmal disease the examination revealed an aneurysm of the anterior communicating artery (diameter, 4 mm; Fig. 1).

Cardiovascular MR imaging

The applied MR angiographic approach yielded diagnostic image quality for all the ten volunteers and five patients. The examination allowed the display of the arterial vasculature from the carotid arteries to the trifurcation vessels during a single injection of gadolinium-based contrast agent within 72 s. A high-grade stenosis of the right renal artery was detected in a 42-year-old male volunteer with known renal artery stenosis (Fig. 2).

The cardiac MR examination revealed a previously unknown myocardial infarction in the apicoseptal region in a 53-year-old man (Fig. 3), demonstrated by late enhancement. Myocardial contractility was slightly compromised in the affected region.

Pulmonary disease

The HASTE data sets revealed four pulmonary lesions ranging in diameter between 3 and 7 mm in one volunteer (n=1) and two patients (n=3). All lesions were diagnosed as granulomas.

MR colonography

Two polyps (diameter 5 and 13 mm) were detected in two patients (Figs. 4, 5). Both lesions, known before, were again confirmed by conventional colonoscopy and subsequent polypectomy was performed.

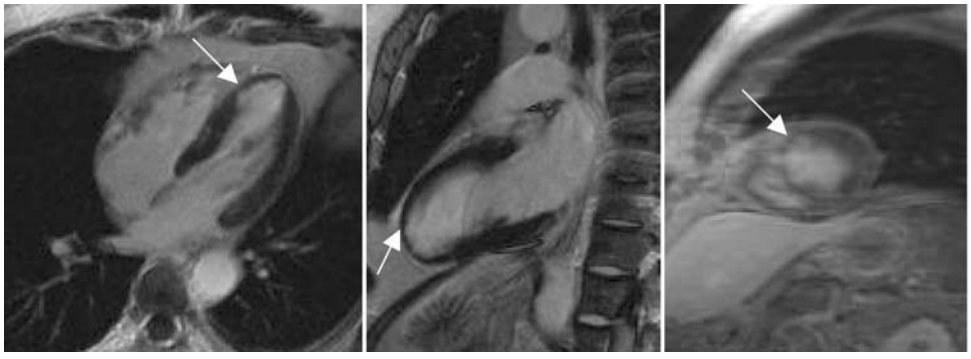

Fig. 3 MR imaging of the heart in a 53-year-old patient with a history of myocardial infarction: "late enhancement" study in long and short axis reveals high signal within the subendocardial apicoseptal myocardium (*arrows*)

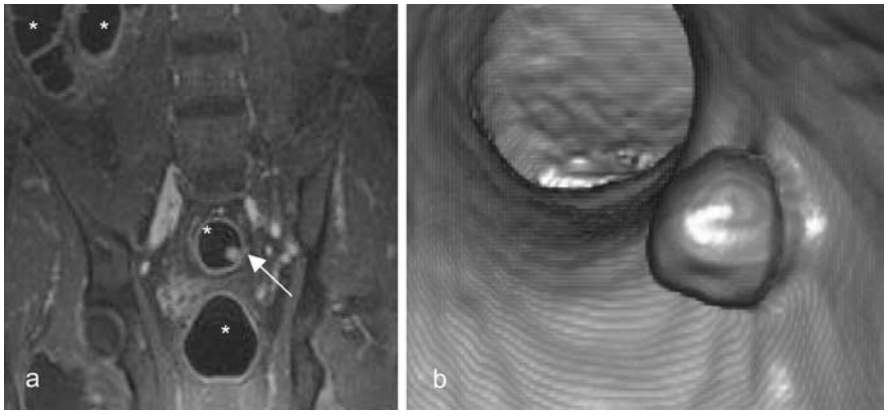

Fig. 4a, b Coronal source image of the 3D MR colonography data set of a 54-year-old male patient with a colorectal polyp confirmed by conventional colonography. The image depicts the colonic wall (*asterisk*) with a small intraluminal contrast-enhancing lesion in the sigmoid **a** (*arrow*); the endoscopic view resulting from the same data set **b** illustrates the polyp to a better extent

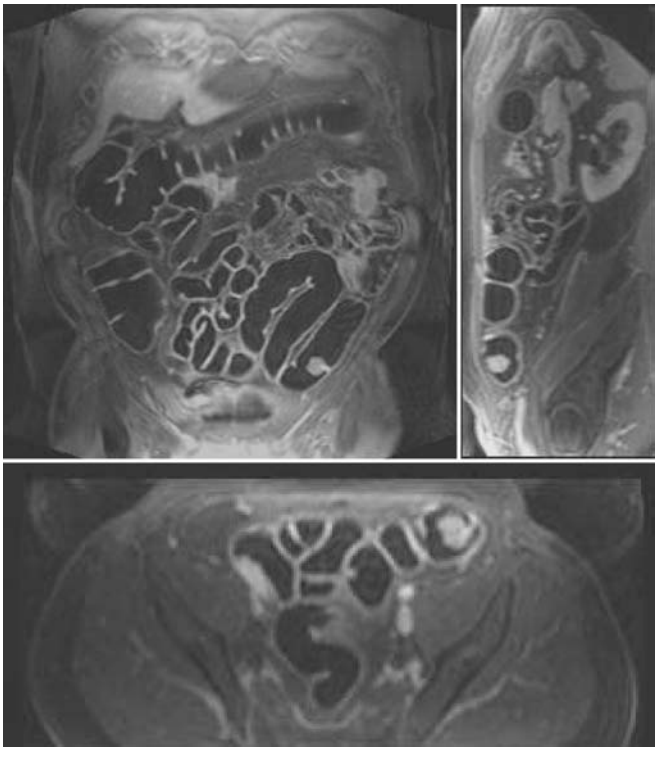

Fig. 5 Coronal source image of the 3D MR colonography data set (coronal, sagittal, axial) of a 63-year-old male patient depicting a 13-mm large polyp in the sigmoid. The diagnosis was confirmed by subsequent conventional colonoscopy and polypectomy was performed

Discussion

The outlined MR screening strategy encompassing the brain, the arterial system, the heart, the lung, and the colon is feasible. Based on the latest high-performance gradients and a sliding table concept, the examination can indeed be completed in little more than 1 h. Image quality is sufficient to readily detect pathologies in the targeted organ systems.

The design of any imaging-based screening strategy must fulfill a number of requirements. First and foremost, diseases affecting the targeted organ systems need to be prevalent and therapeutic interventions at an early stage must be able to prevent morbidity and/or mortality. This of course requires the targeted disease to be detectable by the imaging modality under consideration. Furthermore, the screening examination itself should be easy to tolerate

and not associated with harmful side effects. The proposed comprehensive MR-based strategy fulfills these requirements: (1) the targeted diseases are common and potentially lethal; (2) the MR examination is both sensitive and specific regarding identification of the target diseases; (3) lack of harmful side effects and an overall examination time of little more than 60 min assure high acceptance by individuals undergoing the test.

Cardiovascular disease is the leading cause of mortality in western societies [18]. Despite vast efforts to improve treatment of patients with ischemic heart disease, published results of the WHO MONICA Project show that in industrialized nations about 50% of patients with acute myocardial infarction still die within the first month of the event [19]. These numbers underscore the need for focusing on primary prevention to achieve real further reduction in coronary heart disease mortality rates [19–21]. Accordingly, expert panels in Europe and North America have advocated targeting high-risk individuals for primary prevention [22]. Risk factors predicting cardiovascular events include systemic hypertension, cigarette smoking, elevated levels of total and LDL cholesterol and triglycerides as well as low levels of HDL cholesterol, and diabetes mellitus [19]. While all of these risk factors are readily identifiable by a combination of physical examination, laboratory analysis, and patient history, the proposed MR imaging protocol offers a unique opportunity to assess what damage if any has already been inflicted on the cardiovascular system.

The outlined protocol has been shown to be highly sensitive regarding the identification of pathologies in the cerebrum. The size, number, and distribution of ischemic brain areas permit consideration of possible etiologies: thus microangiopathic changes of the cerebral white matter are highly suggestive of hypertension [23]. Similarly, the proposed protocol offers a highly accurate assessment of myocardial viability. Based on delayed enhancement, infarcted myocardium is detected on T1-weighted images with high sensitivity and specificity [24, 25]. In contrast to existing scintigraphic methods, MR imaging even permits the identification of nontransmural subendocardial infarcts. Furthermore, MR imaging offers the most accurate assessment of left and right ventricular ejection fractions, cardiac mass, and valvular function [26]. In addition, short-axis cine-MR imaging permits evaluation of myocardial contractility both under resting and stress conditions. The latter was not incorporated into the MR protocol presented as it would have prolonged the examination by at least 30 min and would have rendered subsequent MR imaging impossible due to patient agitation.

The cardiovascular screening component also encompasses intracerebral TOF MR angiography and contrast-enhanced multistation whole-body MR angiography. The quality of the former is sufficient to detect small aneurysms or precursors thereof, as shown in one of the screened patients. Whole-body MR angiography mirrors the generalized nature of atherosclerotic disease from a diagnostic viewpoint. The technique has been shown to be highly accurate in the detection and characterization of arterial disease [12, 27]. A stenosis in the carotid artery was identified as readily as a renal artery stenosis. Only the coronary arteries remain unassessed by MR angiography. While several techniques have been proposed, none has gained clinical relevance. This reflects the small size of the coronaries as much as the severe cardiac motion. Although the ability to analyze myocardial viability in combination with ventricular function reduces the impact of this deficit, it would be highly desirable to incorporate coronary MR angiography into a future screening protocol.

Another focus of the proposed MR-based screening protocol relates to the detection of lung and colorectal cancer. MR imaging of the lung had been handicapped by susceptibility effects at the interfaces between pulmonary interstitium and air-filled alveoli. These artifacts can be overcome by using ultrashort echo times [28]. Based on such sequences the accuracy of MR imaging regarding the detection of pulmonary lesions has been shown to be quite high [29, 30]. In a study involving 30 patients with known pulmonary masses, axial HASTE images demonstrated 1,032 of 1,102 lesions seen on CT [31]. Reflecting the lack of signal-providing protons, smaller calcified nodules were missed. Furthermore, lesions with a diameter of less than 3 mm were also missed. All other lesions were clearly detected.

Colorectal cancer has been a focus of screening efforts for quite some time. Despite these efforts, the incidence of colorectal cancer continues to increase with more than 130,000 newly diagnosed patients and 50,000 deaths in the United States alone [32]. The vast majority of colon cancers develop from nonmalignant colonic adenomas or polyps. Thus, cancer-screening programs targeting precancerous colonic polyps with subsequent endoscopic polypectomy are able to reduce cancer mortality by more than 80%. Colorectal screening for polyps may hence be considered one of the most promising preventive measures in medicine [32].

MR colonography overcomes many of the short-comings limiting the clinical impact of existing screening techniques including the gold standard “conventional colonoscopy.” In the setting of a dark, water-filled colonic lumen, it is based on enhancement of the colonic wall as well as of colorectal masses [15, 33]. The technique has been shown to be both sensitive and specific regarding the detection of colorectal masses.

Analysis of the parenchymal organs in the abdomen can be based on 3D gradient-echo data sets collected in the arterial, portal venous, and hepatic venous phases. While the first data set is provided as part of the whole-body MR angiographic examination, the subsequent data sets are collected for MR colonography. Previous studies

have shown this type of dynamic contrast-enhanced 3D imaging of the abdomen to be very accurate regarding the identification of pathologies in the parenchymal organs [34]. Similar experiences have been reported based on MR colonography data sets alone [35].

Clearly, the limited number of individuals included in this study cannot provide relevant data regarding the value of MR-based screening from a societal perspective. This will be accomplished in large-scale studies currently in planning. Rather, the purpose of this paper was to demonstrate the technical feasibility of a comprehensive MR-based screening approach capable of assessing multiple organ systems in a single examination.

The diagnostic accuracy of the different components making up the comprehensive MR imaging protocol has been established in a number of comparative examinations against gold standards. Lack of follow-up examinations in individuals void of pathologic findings prohibits any meaningful analysis in this regard.

To our knowledge, this is the first attempt to implement and evaluate a comprehensive MR-based screening examination. Previous attempts at screening have focused mainly on CT [36]. Particularly, the development of multislice CT has given rise to intensive consideration regarding the use of this technology for assessing cardiovascular risks with coronary calcium scoring [37], lung cancer [4, 5], as well as colorectal cancer with virtual CT colonography [38]. Recently, even whole-body CT screening is being offered on a commercial basis in the United States. Medical professionals are predicting that 5 years from now, there could be as many as 4,000 facilities in the United States alone [6]. All of these approaches, particularly "whole-body CT," are burdened by a considerable exposure to ionizing radiation. This concern prompted the FDA to issue the following statement in April 2002 [7]: "A CT examination with an effective dose of 10 mSv may be associated with an increase in the possibility of fatal cancer of approximately one chance in 2000… nevertheless, this small increase in radiation-associated cancer risk for an individual can become a public health concern if large numbers of the population undergo CT screening." Accordingly, the American College of Radiology, the American College of Cardiology, and the American Heart Association do not recommend CT screening [7].

Compared to the radiation exposure caused by CT, public health concern associated with MR imaging is minimal. Thus, patient exposure to magnetic resonance has never been associated with any harmful side effects [39]. Side effects may, however, be associated with the administration of paramagnetic contrast agents, which must be considered an integral part of the proposed examination. Although rare, anaphylactoid reactions may occur. Hence individuals undergoing the examination need to be carefully monitored. On the other hand, nephrotoxicity, a worry with iodinated contrast agents, is of no concern [40]. Gadobutrol is approved for CNS imaging and MR angiography. As in many other studies, it was in part used in an off-label manner.

We conclude that the outlined MR-based screening strategy encompassing the brain, the arterial system, the heart, the lung, and the colon is feasible and could thus play a pivotal role as part of a comprehensive screening strategy. Further studies have to show whether such MR-based screening programs can indeed be cost-effective in terms of life-years saved.

References

1. Cordes L, Heine F, Krickau G (1972) Results of mass radiography for tuberculosis in older school children. Offentl Gesundheitswes 34:173–179
2. Lunn JA, Mayho V (1989) Incidence of pulmonary tuberculosis by occupation of hospital employees in the National Health Service in England and Wales 1980–1984. J Soc Occup Med 39:30–32
3. Henschke CI, McCauley DI, Yankelevitz DF et al (1999) Early Lung Cancer Action Project: overall design and findings from baseline screening. Lancet 354:99–105
4. Diederich S, Wormanns D, Semik M et al (2002) Screening for early lung cancer with low-dose spiral CT: prevalence in 817 asymptomatic smokers. Radiology 222:773–778
5. Ellis JR, Gleeson FV (2002) New concepts in lung cancer screening. Curr Opin Pulm Med 8:270–274
6. Elsberry RB (2002) The invasion of the body scanners decisions in imaging economics 2002 Feb: 18–21, p 42
7. Whole body scanning using Computed Tomography 17 April 2002 (http://www.fda.gov/cdrh/ct/ FDA)
8. Radiation protection environment DG—Annual Report 2000 (http://europa.eu.int/comm/environment/radprot/anrep_2000.pdf)
9. Lauenstein TC, Freudenberg LS, Goehde SC et al (2002) Whole-body MRI using a rolling table platform for the detection of bone metastases. Eur Radiol 12:2091–2099
10. Gohde SC, Goyen M, Forsting M, Debatin JF (2002) Prevention without radiation—a strategy for comprehensive early detection using magnetic resonance tomography (Article in German). Radiologe 42:622–629
11. Ruehm SG, Goyen M, Barkhausen J et al (2001) Rapid magnetic resonance angiography for detection of atherosclerosis. Lancet 357:1086–1091
12. Goyen M, Quick HH, Debatin JF et al (2002) Whole body 3D MR angiography using a rolling table platform: initial clinical experience. Radiology 224:270–277
13. Ruehm SG, Goyen M, Quick HH et al (2000) Whole-body MRA on a rolling table platform (AngioSURF). RöFo 172:670–674
14. Goyen M, Herborn CU, Lauenstein TC, Debatin JF, Bosk S, Ruehm SG (2002) Optimization of contrast dosage for gadobenate dimeglumine-enhanced high-resolution whole body 3D MR Angiography. Invest Radiol 37:263–268

15. Lauenstein TC, Herborn CU, Vogt FM, Gohde SC, Debatin JF, Ruehm SG (2001) Dark lumen MR-colonography: initial experience. Rofo Fortschr Geb Rontgenstr Neuen Bildgeb Verfahr 173:785–789
16. Vogler H, Platzek J, Schuhmann-Giampieri G et al (1995) Pre-clinical evaluation of gadobutrol: a new, neutral, extracellular contrast agent for magnetic resonance imaging. Eur J Radiol 21:1–10
17. Goyen M, Lauenstein TC, Herborn CU, Debatin JF, Bosk S, Ruehm SG (2001) 0.5 M Gd-Chelate (Magnevist) vs. 1.0 M Gd-Chelate (Gadovist): dose-independent effect on image quality of pelvic 3D MRA. J Magn Res Imaging 14:602–607
18. Anderson KM, Wilson PWF, Odell PM, Kannel WB (1991) An updated coronary risk profile: a statement for health professionals. Circulation 83:356–362
19. Chambless L, Keil U, Dobson A et al (1997) Population versus clinical view of case fatality from acute coronary heart disease—results from the WHO Monica project 1985–1990. Circulation 96:3849–3859
20. Fuster V, Pearson TA (1996) 27th Bethesda Conference. Matching the intensity of risk factor management with the hazard for coronary heart disease events. J Am Coll Cardiol 27:957–1047
21. Anderson KM, Wilson PWF, Odell PM, Kannel WB (1991) An updated coronary risk profile: a statement for health professionals. Circulation 83:356–362
22. Pyorala K, De Backer G, Graham I, Poole-Wilson P, Wood D (1994) On behalf of the task force: prevention of coronary artery disease in clinical practice. Recommandations of the task force of the European Society of Cardiology, European Atherosclerosis Society and European Society of Hypertension. Eur Heart J 15:1300–1331
23. Kim DE, Bae HJ, Lee SH, Kim H, Yoon BW, Roh JK (2002) Gradient echo magnetic resonance imaging in the prediction of hemorrhagic vs ischemic stroke: a need for the consideration of the extent of leukoariosis. Arch Neurol 59:425–429
24. Gerber BL, Lima JA, Garot J, Bluemke DA (2000) Magnetic resonance imaging of myocardial infarct. Top Magn Reson Imaging 11:372–382
25. Barkhausen J, Ebert W, Debatin JF, Weinmann HJ (2002) Imaging of myocardial infarction: comparison of magnevist and gadophrin-3 in rabbits. J Am Coll Cardiol 39(8):1392–1398
26. Barkhausen J, Ruehm SG, Goyen M, Buck T, Laub G, Debatin JF (2001) MR evaluation of ventricular function: true fast imaging with steady-state precession versus fast low-angle shot cine MR imaging: feasibility study. Radiology 219:264–269
27. Goyen M, Herborn CU, Kroger K et al (2003) Detection of atherosclerosis: systemic imaging for systemic disease with whole body three-dimensional MR-angiography—initial experience. Radiology 227:277–282
28. Goyen M, Laub G, Ladd ME, Debatin JF, Barkhausen J, Truemmler KH, Bosk S, Ruehm SG (2001) Dynamic 3D MR angiography of the pulmonary arteries in under 4 seconds. J Magn Res Imaging 13:372–377
29. Kersjes W, Mayer E, Buchenroth M, Schunk K, Fouda N, Cagil H (1997) Diagnosis of pulmonary metastases with turbo-SE MR imaging. Eur Radiol 7:1190–1194
30. Lutterbey G, Leutner C, Gieseke J et al (1998) Detection of focal lung lesions with magnetic resonance tomography using T2-weighted ultrashort turbo-spin-echo-sequence in comparison with spiral computerized tomography. Rofo Fortschr Geb Rontgenstr Neuen Bildgeb Verfahr 169:365–369
31. Schroeder T, Ruehm SG, Ladd ME et al (2002) Detection of pulmonary lesions: MRT Haste vs MultiSlice CT. Proc Intl Soc Mag Reson Med 10:39
32. Landis SH, Murray T, Bodden S, Wingo PA (1998) Cancer statistics. CA Cancer J Clin 48:6–29
33. Papanikolaou N, Grammatikakis J, Maris T, Lauenstein T, Prassopoulos, Goutsoyiannis N (2003) MR colonography with fecal tagging: comparison between 2D turbo FLASH and 3D FLASH sequences. Eur Radiol 13:448–452
34. Hawighorst H, Schoenberg SO, Knopp MV, Essig M, Miltner P, van Kaick G (1999) Hepatic lesions: morphologic and functional characterization with multiphase breath-hold 3D gadolinium-enhanced MR angiography—initial results. Radiology 210:89–96
35. Luboldt W, Bauerfeind P, Steiner P, Fried M, Krestin GP, Debatin J (1997) Preliminary assessment of three-dimensional magnetic resonance imaging for various colonic disorders. Lancet 349(9061):1288–1291
36. Schoepf UJ, Becker CR, Obuchowski NA et al (2001) Multi-slice computed tomography as a screening tool for colon cancer, lung cancer and coronary artery disease. Eur Radiol 11:1975–1985
37. Goldin JG, Yoon HC, Greaser LE III et al (2000) Spiral versus electron-beam CT for coronary artery calcium scoring. Radiology 221:213–221
38. Laghi A, Iannaccone R, Carbone I et al (2002) Detection of colorectal lesions with virtual computed tomographic colonography. Am J Surg 183:124–131
39. Ahmed S, Shellock FG (2001) Magnetic resonance imaging safety: implications for cardiovascular patients. J Cardiovasc Magn Reson 3:171–182
40. Tombach B, Bremer C, Reimer P et al (2001) Renal tolerance of a neutral gadolinium chelate (gadobutrol) in patients with chronic renal failure: results of a randomized study. Radiology 218:651–657